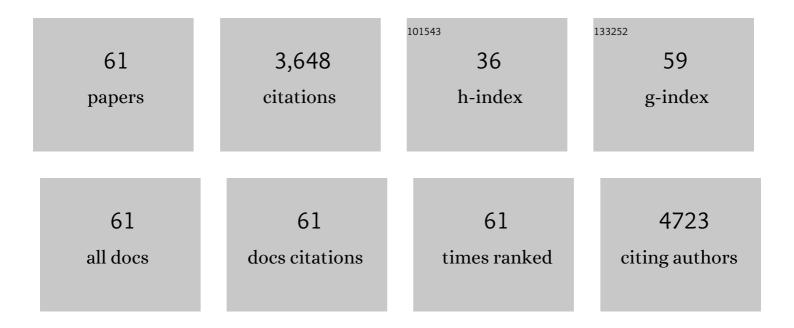
List of Publications by Year in descending order

Source: https://exaly.com/author-pdf/2089419/publications.pdf Version: 2024-02-01



IOHN L FULTON

#	Article	IF	CITATIONS
1	Ionic Contraction across the Lanthanide Series Decreases the Temperature-Induced Disorder of the Water Coordination Sphere. Inorganic Chemistry, 2022, 61, 287-294.	4.0	10
2	Speciation of Cu-Oxo Clusters in Ferrierite for Selective Oxidation of Methane to Methanol. Chemistry of Materials, 2022, 34, 4355-4363.	6.7	11
3	Metal-organic framework supported single-site nickel catalysts for butene dimerization. Journal of Catalysis, 2022, 413, 176-183.	6.2	9
4	Near-Quantitative Predictions of the First-Shell Coordination Structure of Hydrated First-Row Transition Metal Ions Using K-Edge X-ray Absorption Near-Edge Spectroscopy. Journal of Physical Chemistry Letters, 2022, 13, 6323-6330.	4.6	6
5	Structural Characteristics of Amorphous Calcium Sulfate: Evidence to the Role of Water Molecules. Journal of Physical Chemistry C, 2021, 125, 3415-3420.	3.1	19
6	Coordination Sphere of Lanthanide Aqua Ions Resolved with Ab Initio Molecular Dynamics and X-ray Absorption Spectroscopy. Inorganic Chemistry, 2021, 60, 3117-3130.	4.0	33
7	Environment of Metal–O–Fe Bonds Enabling High Activity in CO <sub>2</sub> Reduction on Single Metal Atoms and on Supported Nanoparticles. Journal of the American Chemical Society, 2021, 143, 5540-5549.	13.7	54
8	Materials Engineering of Violin Soundboards by Stradivari and Guarneri. Angewandte Chemie, 2021, 133, 19293-19303.	2.0	6
9	Materials Engineering of Violin Soundboards by Stradivari and Guarneri. Angewandte Chemie - International Edition, 2021, 60, 19144-19154.	13.8	11
10	Activity of Cu–Al–Oxo Extra-Framework Clusters for Selective Methane Oxidation on Cu-Exchanged Zeolites. Jacs Au, 2021, 1, 1412-1421.	7.9	21
11	Frontispiece: Materials Engineering of Violin Soundboards by Stradivari and Guarneri. Angewandte Chemie - International Edition, 2021, 60, .	13.8	0
12	Frontispiz: Materials Engineering of Violin Soundboards by Stradivari and Guarneri. Angewandte Chemie, 2021, 133, .	2.0	0
13	Quantifying the hydration structure of sodium and potassium ions: taking additional steps on Jacob's Ladder. Physical Chemistry Chemical Physics, 2020, 22, 10641-10652.	2.8	38
14	Copper-zirconia interfaces in UiO-66 enable selective catalytic hydrogenation of CO2 to methanol. Nature Communications, 2020, 11, 5849.	12.8	86
15	Understanding the Role of Surface Heterogeneities in Electrosynthesis Reactions. IScience, 2020, 23, 101814.	4.1	16
16	Nanometer-Scale Correlations in Aqueous Salt Solutions. Journal of Physical Chemistry Letters, 2020, 11, 2598-2604.	4.6	10
17	Inverse iron oxide/metal catalysts from galvanic replacement. Nature Communications, 2020, 11, 3269.	12.8	31
18	Importance of Methane Chemical Potential for Its Conversion to Methanol on Cuâ€Exchanged Mordenite. Chemistry - A European Journal, 2020, 26, 7563-7567.	3.3	31

#	Article	IF	CITATIONS
19	Aqueous phase catalytic and electrocatalytic hydrogenation of phenol and benzaldehyde over platinum group metals. Journal of Catalysis, 2020, 382, 372-384.	6.2	68
20	Quantifying Adsorption of Organic Molecules on Platinum in Aqueous Phase by Hydrogen Site Blocking and in Situ X-ray Absorption Spectroscopy. ACS Catalysis, 2019, 9, 6869-6881.	11.2	40
21	Selective Methane Oxidation to Methanol on Cu-Oxo Dimers Stabilized by Zirconia Nodes of an NU-1000 Metal–Organic Framework. Journal of the American Chemical Society, 2019, 141, 9292-9304.	13.7	131
22	Formation of Active Cu-oxo Clusters for Methane Oxidation in Cu-Exchanged Mordenite. Journal of Physical Chemistry C, 2019, 123, 8759-8769.	3.1	60
23	Operando XAFS Studies on Rh(CAAC)-Catalyzed Arene Hydrogenation. ACS Catalysis, 2019, 9, 4106-4114.	11.2	46
24	Many-Body Effects Determine the Local Hydration Structure of Cs <sup>+</sup> in Solution. Journal of Physical Chemistry Letters, 2019, 10, 406-412.	4.6	45
25	Anticorrelated Contributions to Pre-edge Features of Aluminate Near-Edge X-ray Absorption Spectroscopy in Concentrated Electrolytes. Journal of Physical Chemistry Letters, 2018, 9, 2444-2449.	4.6	9
26	Supersaturated calcium carbonate solutions are classical. Science Advances, 2018, 4, eaao6283.	10.3	116
27	Elementary Steps of Faujasite Formation Followed by in Situ Spectroscopy. Chemistry of Materials, 2018, 30, 888-897.	6.7	29
28	Sinterâ€Resistant Platinum Catalyst Supported by Metal–Organic Framework. Angewandte Chemie - International Edition, 2018, 57, 909-913.	13.8	88
29	Carbon-supported Pt during aqueous phenol hydrogenation with and without applied electrical potential: X-ray absorption and theoretical studies of structure and adsorbates. Journal of Catalysis, 2018, 368, 8-19.	6.2	49
30	Well-Defined Rhodium–Gallium Catalytic Sites in a Metal–Organic Framework: Promoter-Controlled Selectivity in Alkyne Semihydrogenation to <i>E</i> -Alkenes. Journal of the American Chemical Society, 2018, 140, 15309-15318.	13.7	88
31	Contact ion-pair structure in concentrated cesium chloride aqueous solutions: An extended X-ray absorption fine structure study. Journal of Electron Spectroscopy and Related Phenomena, 2018, 229, 20-25.	1.7	7
32	Rh(CAAC)-Catalyzed Arene Hydrogenation: Evidence for Nanocatalysis and Sterically Controlled Site-Selective Hydrogenation. ACS Catalysis, 2018, 8, 8441-8449.	11.2	94
33	Atomic Layer Deposition in a Metal–Organic Framework: Synthesis, Characterization, and Performance of a Solid Acid. Chemistry of Materials, 2017, 29, 1058-1068.	6.7	45
34	Methane Oxidation to Methanol Catalyzed by Cu-Oxo Clusters Stabilized in NU-1000 Metal–Organic Framework. Journal of the American Chemical Society, 2017, 139, 10294-10301.	13.7	282
35	Tracking the Chemical Transformations at the BrĄ̃nsted Acid Site upon Water-Induced Deprotonation in a Zeolite Pore. Chemistry of Materials, 2017, 29, 9030-9042.	6.7	71
36	Bridging Zirconia Nodes within a Metal–Organic Framework via Catalytic Ni-Hydroxo Clusters to Form Heterobimetallic Nanowires. Journal of the American Chemical Society, 2017, 139, 10410-10418.	13.7	74

#	Article	IF	CITATIONS
37	High-resolution Measurement of Contact Ion-pair Structures in Aqueous RbCl Solutions from the Simultaneous Corefinement of their Rb and Cl K-edge XAFS and XRD Spectra. Journal of Solution Chemistry, 2016, 45, 1061-1070.	1.2	9
38	Sintering-Resistant Single-Site Nickel Catalyst Supported by Metal–Organic Framework. Journal of the American Chemical Society, 2016, 138, 1977-1982.	13.7	273
39	Glucose―and Celluloseâ€Derived Ni/Câ€SO <sub>3</sub> H Catalysts for Liquid Phase Phenol Hydrodeoxygenation. Chemistry - A European Journal, 2015, 21, 1567-1577.	3.3	14
40	Determination of the Dominant Catalyst Derived from the Classic [RhCp*Cl <sub>2</sub> ] <sub>2</sub> Precatalyst System: Is it Single-Metal Rh <sub>1</sub> Cp*-Based, Subnanometer Rh <sub>4</sub> Cluster-Based, or Rh(0) <i><sub>n</sub></i> Nanoparticle-Based Cyclohexene Hydrogenation Catalysis at Room Temperature and Mild Pressures?. ACS Catalysis, 2015, 5,	11.2	28
41	2876-3886 Electronic and Chemical State of Aluminum from the Single- (K) and Double-Electron Excitation (KL <sub>Il&amp;III</sub> , KL <sub>I</sub> ) X-ray Absorption Near-Edge Spectra of α-Alumina, Sodium Aluminate, Aqueous Al <sup>3+</sup> ·(H <sub>2</sub> O) <sub>6</sub> , and Aqueous Al(OH) <sub>4</sub> <sup>–</sup> . Iournal of Physical Chemistry B. 2015, 119, 8380-8388.	2.6	20
42	Impact of Zeolite Aging in Hot Liquid Water on Activity for Acid-Catalyzed Dehydration of Alcohols. Journal of the American Chemical Society, 2015, 137, 10374-10382.	13.7	63
43	State of Supported Nickel Nanoparticles during Catalysis in Aqueous Media. Chemistry - A European Journal, 2015, 21, 16541-16546.	3.3	14
44	Quantitatively Probing the Al Distribution in Zeolites. Journal of the American Chemical Society, 2014, 136, 8296-8306.	13.7	199
45	State of Supported Pd during Catalysis in Water. Journal of Physical Chemistry C, 2013, 117, 17603-17612.	3.1	43
46	lon-pairing in aqueous CaCl2 and RbBr solutions: Simultaneous structural refinement of XAFS and XRD data. Journal of Chemical Physics, 2013, 138, 044201.	3.0	39
47	The Aqueous Ca <sup>2+</sup> System, in Comparison with Zn <sup>2+</sup> , Fe <sup>3 +</sup> , and Al <sup>3 +</sup> : An Abâ€Initio Molecular Dynamics Study. Chemistry - A European Journal, 2013, 19, 3047-3060.	3.3	45
48	Near-Quantitative Agreement of Model-Free DFT-MD Predictions with XAFS Observations of the Hydration Structure of Highly Charged Transition-Metal Ions. Journal of Physical Chemistry Letters, 2012, 3, 2588-2593.	4.6	40
49	A variable ultra-short-pathlength solution cell forÂXAFS transmission spectroscopy of light elements. Journal of Synchrotron Radiation, 2012, 19, 949-953.	2.4	8
50	ls It Homogeneous or Heterogeneous Catalysis Derived from [RhCp*Cl <sub>2</sub> ] <sub>2</sub> ? <i>In Operando</i> XAFS, Kinetic, and Crucial Kinetic Poisoning Evidence for Subnanometer Rh <sub>4</sub> Cluster-Based Benzene Hydrogenation Catalysis. Journal of the American Chemical Society, 2011, 133, 18889-18902.	13.7	147
51	Structure of Hydronium (H <sub>3</sub> O <sup>+</sup> )/Chloride (Cl <sup>â^'</sup> ) Contact Ion Pairs in Aqueous Hydrochloric Acid Solution: A Zundel-like Local Configuration. Journal of the American Chemical Society, 2010, 132, 12597-12604.	13.7	47
52	Hydrated Structure of Ag(I) Ion from Symmetry-Dependent, K- and L-Edge XAFS Multiple Scattering and Molecular Dynamics Simulations. Journal of Physical Chemistry A, 2009, 113, 13976-13984.	2.5	51
53	Defining Active Catalyst Structure and Reaction Pathways from ab Initio Molecular Dynamics and Operando XAFS: Dehydrogenation of Dimethylaminoborane by Rhodium Clusters. Journal of the American Chemical Society, 2009, 131, 10516-10524.	13.7	67
54	Molecular Simulation Analysis and X-ray Absorption Measurement of Ca2+, K+and Cl-Ions in Solution. Journal of Physical Chemistry B, 2006, 110, 23644-23654.	2.6	115

#	Article	IF	CITATIONS
55	Hydration and contact ion pairing of Ca2+ with Clâ^' in supercritical aqueous solution. Journal of Chemical Physics, 2006, 125, 094507.	3.0	41
56	High-pressure, high-temperature x-ray absorption fine structure transmission cell for the study of aqueous ions with low absorption-edge energies. Review of Scientific Instruments, 2004, 75, 5228-5231.	1.3	18
57	Understanding the Effects of Concentration on the Solvation Structure of Ca2+ in Aqueous Solution. I:  The Perspective on Local Structure from EXAFS and XANES. Journal of Physical Chemistry A, 2003, 107, 4688-4696.	2.5	201
58	An X-ray absorption fine structure study of copper(I) chloride coordination structure in water up to 325°C. Chemical Physics Letters, 2000, 330, 300-308.	2.6	95
59	Copper(I) and Copper(II) Coordination Structure under Hydrothermal Conditions at 325 °C:  An X-ray Absorption Fine Structure and Molecular Dynamics Study. Journal of Physical Chemistry A, 2000, 104, 11651-11663.	2.5	117
60	A Transition in the Ni2+ Complex Structure from Six- to Four-Coordinate upon Formation of Ion Pair Species in Supercritical Water:  An X-ray Absorption Fine Structure, Near-Infrared, and Molecular Dynamics Study. Journal of Physical Chemistry A, 1999, 103, 8471-8482.	2.5	91
61	Direct Modeling of EXAFS Spectra from Molecular Dynamics Simulations. The Journal of Physical Chemistry, 1996, 100, 13393-13398.	2.9	129